Renewable Energy 243 (2025) 122516

Contents lists available at ScienceDirect

Renewable Energy

journal homepage: www.elsevier.com/locate/renene

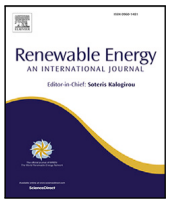

# Swarm intelligence-based Multi-Layer Kernel Meta Extreme Learning Machine for tidal current to power prediction

Emrah Dokur [a], Nuh Erdogan [b,*], Ugur Yuzgec [c]

[a] Department of Electrical Electronics Engineering, Faculty of Engineering, Bilecik Seyh Edebali University, Bilecik, Turkiye
[b] Department of Engineering, School of Science and Technology, Nottingham Trent University, Nottingham, UK
[c] Department of Computer Engineering, Faculty of Engineering, Bilecik Seyh Edebali University, Bilecik, Turkiye

ARTICLE INFO

*Keywords:*
Extreme Learning Machine
Forecasting
Ocean renewable energy
Swarm decomposition
Tidal energy

ABSTRACT

Tidal energy, with its predictable and consistent nature, offers a scalable ocean renewable resource that can diversify the energy generation mix for countries with suitable coastal conditions. Accurate tidal current-to-power forecasting is essential to optimize power system management, improve grid stability, and inform the design of power processing and storage units. This study proposes a novel hybrid model integrating Swarm Decomposition with a Multi-Layer Kernel Meta Extreme Learning Machine to forecast non-stationary tidal currents. The Swarm Decomposition isolates key oscillatory components, reducing noise and improving feature extraction, while the kernel-based architecture enhances generalization and scalability by minimizing the need for extensive parameter tuning, resulting in higher forecasting accuracy and computational efficiency. The model is validated on two real-world tidal current datasets from distinct locations, incorporating seasonal variations, and compared against well-established extreme learning machines and deep learning models. A sensitivity analysis of signal decomposition parameters demonstrated their impact on decomposition quality and computational cost. The proposed model outperformed superior performance on both tidal datasets, achieving a 5-fold reduction in mean squared error and increased $R^2$ from 0.9653 to 0.9933. These findings highlight the model's robustness and adaptability to diverse tidal conditions, making it a reliable tool for tidal power forecasting.

## 1. Introduction

Ocean renewable energy is abundant and geographically diverse, comprising a variety of renewable sources, including wave, tidal stream and range, ocean thermal, and offshore wind [1]. In response to the unprecedented strain on global energy supplies in 2022, governments in Europe, the United States, and China are increasingly diversifying their national energy mixes. As part of this effort, ocean energy sources such as tidal and offshore wind are emerging as vital solutions to enhance energy security and autonomy. Among these, tidal energy has attracted significant attention in the past decade, benefiting from technology adapted from the established wind sector [2]. By 2024, the global cumulative capacity of the tidal stream has reached 43.6 MW, contributing to an annual energy production of 93 GWh [3]. This capacity is projected to grow significantly, with an additional 137 MW under development over the next five years, driven by European Union (EU) and national support programs. While the tidal energy is generally predictable, several factors affect the intensity and behavior of tidal currents. Local variabilities and environmental factors, such as coastal geography, seafloor topography, water temperature, and seasonal weather patterns, can influence tidal current strength and create local variations that require precise forecasting for optimal power output predictions [4]. Moreover, short-term, non-periodic influences, such as storms and turbulence, further affect the behavior of the tidal current [5]. For effective grid integration, high-resolution forecasts are essential to synchronize tidal power output with demand patterns, and efficiently design and manage energy storage units [6]. Accurate forecasting models also enable optimized tidal turbine operation, reducing wear, maximizing efficiency, and supporting timely maintenance scheduling to minimize downtime.

The traditional method of harmonic analysis based on the astronomical forces that affect ocean tides for tidal prediction is discussed in [7]. Incorporating observational data into physical models is proposed to improve the predictive accuracy based on current conditions. Similarly, the study in [8] employs harmonic analysis to preprocess tidal data, which is then used with deep learning models, Long short-term memory (LSTM), Gated recurrent unit, and bi-directional Long short-term

* Corresponding author.
*E-mail addresses:* emrah.dokur@bilecik.edu.tr (E. Dokur), nuh.erdogan@ntu.ac.uk (N. Erdogan), ugur.yuzgec@bilecik.edu.tr (U. Yuzgec).

https://doi.org/10.1016/j.renene.2025.122516
Received 1 November 2024; Received in revised form 4 January 2025; Accepted 26 January 2025
Available online 5 February 2025

**Nomenclature**

| | |
|---|---|
| $\delta$ | Flexibility of swarm. |
| $f(\cdot)$ | activation function. |
| $H_j^{(m)}$ and $X_j^{(m)}$ | Output and input matrices for the $j$th subset in the $m$th layer, respectively. |
| $M$ | The number of swarms. |
| $n$ | The number of steps. |
| $P_i$ | Position of $i$th prey. |
| $R^2$ | Coefficient of determination. |
| $V_i$ | Velocity of $i$th prey. |
| $W_j^{(m)}$ and $b_j^{(m)}$ | Weight and bias vectors for the $j$th subset in the $m$th layer, respectively. |
| $\Omega$ | Kernel matrix. |
| ANN | Artificial neural network. |
| ARIMA | Autoregressive integrated moving average. |
| Bi-LSTM | Bi-directional long short-term memory. |
| CEEMDAN | Complete ensemble empirical mode decomposition with adaptive noise. |
| CNN | Convolutional neural network. |
| CV | Coefficient of variation |
| DBN | Deep belief network. |
| ELM | Extreme learning machine. |
| EU | European Union. |
| LSTM | Long short-term memory. |
| MAE | Mean absolute error. |
| ML | Machine learning. |
| ML-MetaKELM | Multi-Layer Kernel Meta Extreme Learning Machine. |
| MLP | Multi-layer perceptron. |
| MSE | Mean squared error. |
| NOAA | National Oceanic and Atmospheric Administration. |
| OC | Oscillatory components. |
| PI | prediction interval. |
| RBF | Radial basis function. |
| RMSE | Root mean squared error. |
| SVT | Support vector regression. |
| SWD | Swarm decomposition. |
| SWF | Swarm filtering. |
| VMD | Variational mode decomposition. |
| WD | Wavelet decomposition. |

memory (Bi-LSTM) to assess the impact of wind on tidal predictions. The results highlight wind as a critical factor in enhancing short-term tidal forecasting accuracy. However, a notable limitation of these deep learning models is their data-intensive nature and longer training times, which can challenge their scalability. In [9], numerical simulations are integrated into deep learning approaches, including Multilayer Perceptron (MLP) and LSTM to correct for tidal velocity errors for high-accuracy tidal current predictions and energy resource assessments. However, the numerical models heavily depend on accurate boundary conditions, such as tidal constituents, bathymetry, and initial conditions, to simulate tidal dynamics. Any inaccuracy in these inputs, such as imprecise bathymetric data or boundary forcing parameters, can result in significant deviations between simulated and real-world tidal behavior. Furthermore, physics-based models are computationally intensive, making it challenging to scale for large regions, high-resolution domains, or long-term simulations. More critically, their performance is highly sensitive to parameter choices – like bottom friction coefficients, vertical mixing schemes, and grid resolution – which can significantly affect simulation fidelity.

To overcome the limitations of traditional methods and better capture complex, nonlinear tidal behaviors, recent research has increasingly adopted machine learning (ML) approaches, which offer flexible, data-driven solutions to forecast water levels and discharges in tidal environments [10]. The study in [11] employs a Deep Neural Network to replace missing tidal data and forecast tidal levels. The proposed method outperforms traditional statistical methods and other artificial neural network (ANN) models for missing value imputation and tidal-level forecasting. However, its robustness in handling highly non-linear and multi-factorial tidal variations is limited, as it lacks mechanisms to isolate complex frequency components and does not consider external environmental factors such as wind, atmospheric pressure, and coastal topography. In [5], the hybrid ARIMA-SVR model utilizes Autoregressive integrated moving average (ARIMA) for linear components and Support vector regression (SVR) for nonlinear dynamics to improve the accuracy of the prediction of tidal currents. While this approach captures some linear–nonlinear interactions, it may struggle with multi-frequency, non-stationary characteristics in highly variable tidal conditions. In addition, its computational demands could limit the scalability for long-term forecasts. In [12] a hybrid forecasting model is proposed that combines ARIMA and Deep Belief Network (DBN) to predict the occurrences of red tide, with ARIMA modeling linear components and DBN capturing non-linear dependencies on environmental factors. Particle Swarm Optimization is used to optimize parameters in both ARIMA and DBN, enhancing training speed and accuracy. Although this approach effectively addresses both linear and nonlinear aspects of red tide data, reliance on ARIMA may reduce flexibility in handling complex, non-stationary fluctuations, potentially limiting forecasting accuracy in highly variable marine environments. The study in [13] employs LSTM to effectively capture the sequential and cyclical nature of tidal data, outperforming traditional models like ARIMA and other ML methods implemented, *i.e.*, ANN, Convolutional neural network (CNN), SVR. However, LSTM may be limited in handling multi-frequency, high-variability tidal patterns in complex tidal environments. Das et al. in [14] introduce an MLP-based model for time-series forecasting, optimized for computational efficiency and effective in long-term forecasting with lower memory requirements. However, it may face challenges in accurately capturing the complex temporal dynamics of tidal environments. The study in [15] introduces a probabilistic approach to forecasting tidal currents with SVR-based prediction intervals (PIs) rather than point forecasts. Constructing PIs increases the computational intensity, which is typical in SVR, limiting the model's practicality for large or high-resolution tidal datasets. Given these limitations in handling multi-frequency and non-stationary tidal characteristics, recent research has increasingly focused on integrating signal decomposition techniques with ML models to better capture the complex temporal dynamics inherent in tidal environments.

Hybrid models integrate various signal processing techniques with conventional or advanced machine learning models to address the nonlinearities and aperiodic behavior inherent the data [16]. While the nonlinearity of tidal streams arises from their complex nature, aperiodic behavior refers to irregular or non-repeating variations caused by factors such as meteorological influences (*e.g.*, storms, wind surges, atmospheric pressure changes), geophysical dynamics (*e.g.*, estuarine conditions and bathymetry), and non-linear interactions with local hydrodynamics (*e.g.*, eddies and turbulence) [17]. In this respect, signal processing methods are used to decompose tidal signals into independent oscillatory components. Isolating these components allows the subsequent forecasting models to focus on specific patterns while reducing the influence of noise and unrelated signals. In [10], hybrid models are presented that integrate wavelet decomposition (WD) and harmonic analysis within ML frameworks to effectively manage non-stationary, multi-frequency tidal data, capturing both high- and low-frequency variations essential to accurately model tidal currents.

Peng et al. [4] decompose tidal current data into periodic and random components using a layered hybrid model, where Hierarchical extreme learning machine (ELM) captures turbulence-induced randomness and LSTM handles periodic trends. This decomposition enhances short-term forecasting accuracy by allowing the model to process predictable and irregular fluctuations independently. The study in [6] incorporates wavelet-based signal decomposition with a Neural Network to enhance tidal current forecasting accuracy. The WD captures oscillatory behavior in tidal data, improving the model's adaptability to both short-term fluctuations and long-term trends. Additionally, k-means clustering organizes the decomposed data into similar patterns, further enhancing forecasting precision by grouping data with similar tidal characteristics. The hybrid model proposed in [18] utilizes CNN's feature extraction capabilities and Bi-LSTM's temporal processing strength. The study employs an improved symplectic geometric mode decomposition to decompose the tidal data into stable sub-components that better represent the non-stationary, complex nature of tidal energy fluctuations. While this multi-stage approach achieves high precision in capturing complex energy patterns, its layered structure and high computational demands may limit scalability and efficiency, particularly for real-time or large-scale forecasting applications. In [19], an uncertainty-aware deep neuroevolution algorithm is proposed to optimize the parameters of a deep learning model (*e.g.*, CNN-LSTM), achieving superior accuracy in tidal level interval forecasting. In [20], the Variational Mode Decomposition (VMD) method is used to decompose the original tidal height time series into frequency-specific components, which an LSTM model individually processes. The predictions for each component are then superimposed and summed, demonstrating superior performance in tidal height prediction compared to single Support vector machine and LSTM models, as well as the CEEMDAN-enhanced LSTM model. Cheng et al. In [21] integrate time-frequency analysis using Discrete Wavelet Transform with a convolutional neural network to model intra-period and inter-period variations in tidal current time series to address the challenges of capturing multiple periodicity in tidal current forecasting. Although this approach significantly improves short-term forecasting accuracy, the wavelet-based analysis is computationally intensive, leading to inefficiencies in processing time. As a result, these decomposition-aided hybrid models have advanced tidal forecasting by effectively capturing both linear and nonlinear components. However, the inherent trade-offs between forecasting accuracy and computational demand indicate the need for further innovation to address the unique complexities of highly dynamic tidal environments.

Despite advances in tidal forecasting methods, significant challenges remain unresolved. Traditional models, such as harmonic analysis, are limited in capturing non-linear and multi-frequency tidal dynamics, while numerical simulations are highly dependent on accurate boundary conditions, which are often difficult to obtain. Hybrid approaches that integrate signal decomposition techniques with ML models offer improved accuracy but are often hindered by increased computational complexity, sensitivity to parameter tuning, and limited scalability for real-time or large-scale applications. Furthermore, there is a gap in models, balancing forecasting accuracy and computational efficiency, particularly when addressing the seasonal and non-stationary variations inherent in tidal environments. In this respect, this study aims to address these challenges by proposing a novel hybrid approach that combines high accuracy with computational scalability while effectively managing the complexities of multi-frequency and seasonal tidal variations. In this study, the following research questions were developed : *(i)* How can tidal forecasting models achieve an optimal balance between high precision and computational scalability? *(ii)* How can a hybrid approach combining Swarm decomposition (SWD) and Multi-Layer Kernel Meta Extreme Learning Machine (ML-MetaKELM) optimize this trade-off? *(iii)* To what extent does the SWD enhance forecasting accuracy by isolating multi-frequency and non-stationary tidal signals? *(iv)* How can modular training in ML-MetaKELM reduce training times while maintaining forecasting accuracy in complex tidal environments?

Building on these advances in the literature, this study introduces a novel hybrid model designed for accurate, reliable, and scalable tidal current-to-power forecasting. In this model, the architecture is designed to balance complexity and computational efficiency in handling diverse datasets. The proposed approach integrates the SWD technique with the proposed ML-MetaKELM model. The structure adopts the strengths of SWD for signal decomposition and ML-MetaKELM for advanced feature learning, providing a smooth integration of data preprocessing and prediction capabilities. The SWD module efficiently decomposes non-stationary tidal signals into distinct oscillatory components, reducing noise and isolating critical features for improved forecasting accuracy. This is complemented by the ML-MetaKELM architecture, which utilizes kernel-based transformations and modular training to improve generalization and accelerate training times. Partitioning data subsets and training each ELM on a different segment reduce the computational time. Such modularity in training enhances adaptability and reduces the burden of hyperparameter optimization. This design enables the model to manage large-scale and non-stationary tidal datasets, while maintaining robust generalization performance. The proposed model is evaluated using two real-world tidal current datasets from geographically distinct locations, capturing seasonal variations, from January, April, July, and October. Its performance is comparatively validated against other ELM-based models and the widely used deep learning model, LSTM, using numerical metrics such as the mean absolute error (MAE), the mean squared error (MSE), the root mean squared error (RMSE), the coefficient of determination ($R^2$), and the coefficient of variation ($CV$). Additionally, a sensitivity analysis is performed to assess the impact of SWD parameters on the quality and computational efficiency of the decomposition process. As such, the robustness of the SWD methodology is demonstrated.

The remainder of this paper is organized as follows: Section 2 describes the proposed methodology and mathematical development of the model; Section 3 presents the analysis of the tidal current datasets used and discusses the results of the testing and validation results including a sensitivity analysis,; and Section 4 provides concluding remarks and future research directions.

## 2. Methodology

### 2.1. Approach

The main architecture of the proposed model consists of three cascaded modules, as presented in Fig. 1. The SWD module is introduced within a Kernel-Based Meta-ELM model to improve tidal current prediction accuracy while maintaining low computational complexity. In the decomposition module, unlike the traditional forecasting models, relying on the singular characteristics of signal, the SWD is applied to capture oscillatory components from non-stationary signals, enabling detailed feature extraction from tidal stream data. This approach improves forecasting accuracy for each sub-component of the data. The Swarm Filtering (SWF) process within SWD optimally extracts oscillatory components, reducing the pseudo-Gibbs phenomenon that typically associated with traditional decomposition methods such as WD. This results in sub-components with richer time-frequency characteristics, which deepens the physical understanding of tidal currents while maintaining computational efficiency. In the forecasting module, the decomposed sub-components feed into the Multi-Layer Kernel based Meta ELM model. The proposed forecasting model addresses key deep learning challenges in feature extraction and representation. While deep ELM models, typically stacking ELM autoencoders [22], have been proposed in the literature, our approach mitigates the need for extensive trial-and-error tuning by employing a simplified architecture. The kernel-based design improves generalization, while the Meta-ELM accelerates training by dividing data into subsets and training each ELM on separate parts. This approach significantly reduces computational

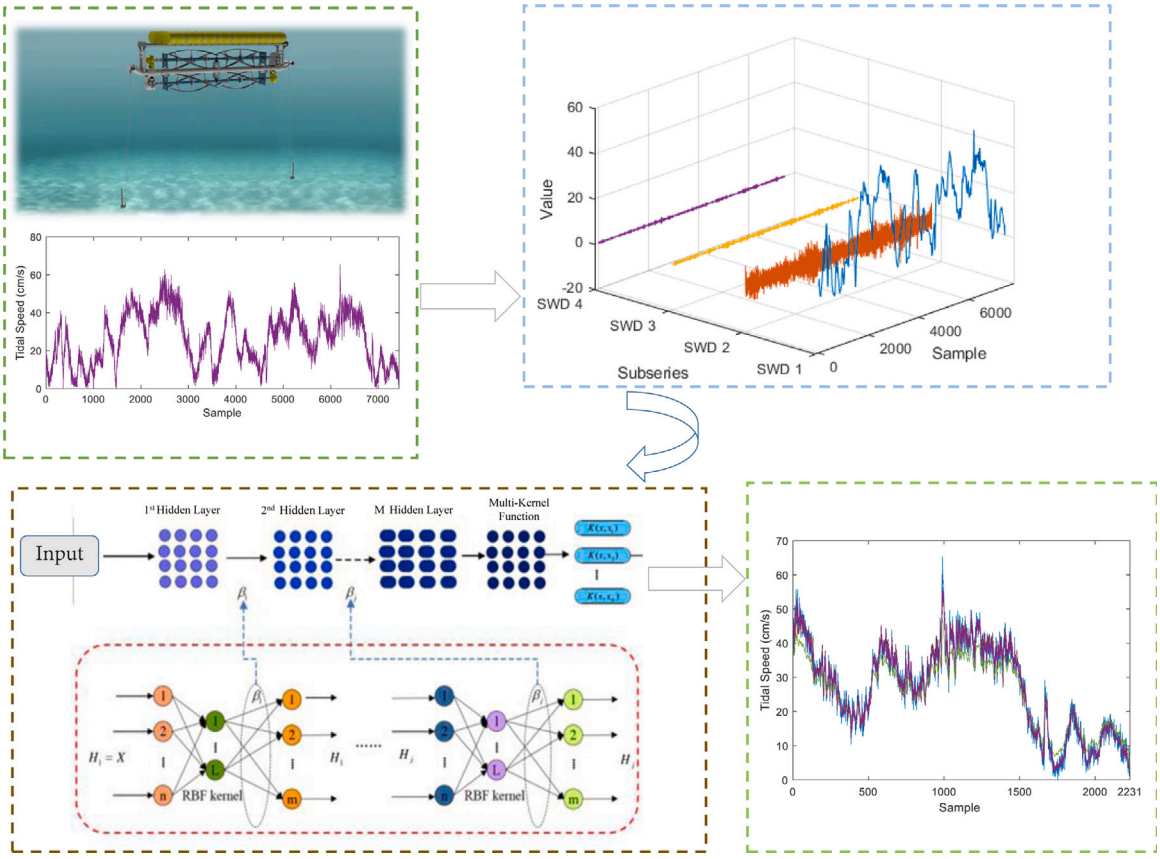


**Fig. 1.** The main framework of the proposed forecasting methodology.

time and enhances forecasting accuracy, making it suitable for complex, non-stationary datasets. Finally, the aggregation module combines individual forecasts from all sub-components, producing a comprehensive tidal current prediction.

### 2.2. The swarm decomposition

The SWD method is an intelligent signal analysis approach designed to decompose nonstationary multi-component signals into their individual oscillatory components (OCs) [23]. It is based on the principles of SWF, which simulates the behavior of a swarm-prey hunting mechanism to iteratively extract oscillatory modes from complex signals. This method adapts swarm intelligence, where a virtual swarm of agents interacts with a dynamic prey, corresponding to the desired components within the signal. SWD aims to efficiently decompose signals by iteratively applying SWF to isolate these components based on their energy spectral density.

The decomposition process begins with the identification of the center frequency of the dominant oscillatory component using the power spectrum of the input signal. The swarm then moves toward this target frequency by calculating both the driving and cohesion forces, which influence the movement of each swarm member. These forces are modeled to ensure that the swarm members co-here around the prey, leading to the isolation of the most prominent oscillatory component in the signal. Once a component is extracted, it is subtracted from the original signal, and the process is repeated for the residual signal until no further significant components are found. If $i$ and $n$ are the number of members and steps, respectively, the driving force $F_{dr}(n,i)$ is defined as follow:

$$F_{dr}(n,i) = P_{prey}(n) - P_i(n-1). \tag{1}$$

The position of the prey is denoted by $P_{prey}$. Unlike the driving force, the cohesion force $F_{Coh,i}$, which represents the interactions among all members, can be calculated by

$$F^n_{Coh,i} = \frac{1}{M-1}.\sum_{j=1,j\neq i}^{M} f(P_i[n-1] - P_j(n-1)), \tag{2}$$

$$f(d) = -sgn(d).\ln\left(\frac{|d|}{d_{cr}}\right), \tag{3}$$

where $M$ represents the number of swarms, and the function $f(.)$ is defined based on the distance between members, $d$, and the critical distance, $d_{cr}$. In this context, $sgn(.)$ and $ln(.)$ correspond to the sign and logarithmic functions, respectively. During the hunting process of the swarm and prey, the members are required to update their positions, $P_i$, and velocities, $V_i$, as follows:

$$V_i[n] = V_i[n-1] + \delta.\left(F^n_{Dr,i} + F^n_{Coh,i}\right), \tag{4}$$

$$P_i[n] = P_i[n-1] + \delta.\left(V_i[n]\right). \tag{5}$$

The parameter $\delta$ is the flexibility of the swarm. Once the hunting process is finished, the output of the SWF can be expressed by

$$y[n] = \beta.\sum_{i=1}^{M} P_i[n], \tag{6}$$

where $\beta$ is the scale parameter that is selected to be 0.005 as in [24]. The output of SWF is influenced by two key parameters: $\delta$ and $M$. These parameters are determined on the basis of the normalized frequency as follows:

$$\arg_{\delta,M}\ min \sum_k \left\{\left|Y_{\delta,M}[k] - |S[k]|\right|\right\}^2, \tag{7}$$

$$M(\hat{\omega}) = [33.46\hat{\omega}^{-0.735} - 29.1], \tag{8}$$

$$\delta(\hat{\omega}) = -1.5\hat{\omega}^2 + 3.454\hat{\omega} - 0.01. \tag{9}$$

The critical factors affecting SWD include the number of swarm members ($M$) and the parameter $\delta$, which influences the flexibility of the swarm. These parameters, along with thresholds used to extract oscillatory components play a significant role in optimizing the decomposition process. The adaptability of SWD enables it to manage signals with varying frequencies and amplitudes efficiently. The integration of the Savitzky-Golay filter enhances the smoothing phase during decomposition, improving computational efficiency by narrowing the search range in frequency selection [25].

### 2.3. Multi-layer kernel meta extreme learning machine (ML-MetaKELM)

The architecture of ELM displays structural similarities with other prominent neural network models, such as Back Propagation Neural Networks and radial basis function networks. Among the various neural network models, ELM has gained recognition as a highly efficient and powerful method [26] due to its unique characteristics, including rapid learning, simple implementation, and strong generalization capability [27]. While ELM achieves fast results by training single-layer artificial neural networks with randomly assigned weights, its precision may be limited in complex problems.

The ML-MetaKELM model presented in this study overcomes the limitations of classical ELM and provides a more powerful and flexible structure. It provides information transfer between layers in a manner similar to deep learning models, using kernel-based transformations at each layer while learning from data divided into subsets. The model adopts an auto-encoder-like approach, where each layer learns progressively higher-level representations of the input data, passing these refined representations to the subsequent layer.

The model has an L-layer structure. In each layer, the data is divided into $M$ subsets and each subset learns its own hidden layer weights and kernel transformation. The outputs of the layers are used as input to the next layer. First, hidden layer weights and bias values are randomly assigned in the meta sub-ELM groups in each layer. With the data sets divided into subsets in the meta-sub-ELM groups, the output weights of these sub-ELM groups are updated by

$$H_j^{(m)} = f\left(X_j^{(m)} W_j^{(m)^\top} + b_j^{(m)}\right), \tag{10}$$

where $H_j^{(m)}$ denotes the output of the hidden layer for the $j$th subset in the $m$th layer, $X_j^{(m)}$ represents the input data matrix for the $j$th subset in the $m$th layer, $W_j^{(m)}$ stands for the weight matrix for the $j$th subset in the $m$th layer, $b_j^{(m)}$ denotes the bias vector for the $j$th subset in the $m$th layer, and $f(\cdot)$ is the activation function. The output weights for each meta-sub-ELM group are obtained using the autoencoder method as follows:

$$\beta_j^{(m)} = H_j^{\dagger(m)} X_j^{(m)}, \tag{11}$$

where $H_j^{\dagger(m)}$ represents the inverse matrix of $H_j^{(m)}$ using Moore–Penrose pseudo-inverse method, $\beta_j^{(m)}$ is the output weights for the $j$th subset in the $m$th layer. For each sub-meta ELM group in the relevant layer, the hidden layer outputs $H^{(m)}$ are calculated for the entire input data set $X^{(m)}$ by

$$H^{(m)} = \sum_{j=1}^{M} \beta_j^{(m)} f\left(X^{(m)} W_j^{(m)^\top} + b_j^{(m)}\right). \tag{12}$$

Then, a kernel matrix $\Omega$ using the kernel function $K$ can be defined by applying Mercer's conditions on each layer output:

$$\Omega^{(m)} = H^{(m)} H^{(m)^\top}, \tag{13}$$

where $\Omega^{(m)}$ equals $K^{(m)}(x_i, x_j) = exp(-\left\|x_i - x_j\right\| / 2{\sigma_m}^2)$. Kernel functions satisfy the Mercer condition, making them suitable for practical applications. Various kernel functions can be considered, such as the polynomial kernel, Gaussian kernel, hyperbolic tangent kernel (Sigmoid kernel), and wavelet kernel [28]. In this study, the kernel of the radial basis function (RBF) is selected for analysis. Depending on the operation of the kernel, the transformation matrix ($\Gamma^{(m)}$) is found as follows:

$$\Gamma^{(m)} = \left(\frac{I}{C^{(m)}} + \Omega^{(m)}\right)^{-1} X^{(m)}, \tag{14}$$

where $I$ represents the unit matrix, $C^{(m)}$ represents the regularization parameter in the $m$th layer. Based on previous research [29,30], a value of 50 is adopted for the $C$ parameter in this study. The input of the next layer $X^{(m+1)}$ is the product of $\Omega^{(m)}$ and $\Gamma^{(m)}$ by

$$X^{(m+1)} = \Omega^{(m)} \cdot \Gamma^{(m)}. \tag{15}$$

These procedures are applied in each layer of ML-MetaKELM until the final layer is reached. The procedures in the last layer of the model are as follows:

$$H_j^{(L)} = f\left(X_j^{(L)} W_j^{(L)^\top} + b_j^{(L)}\right), \tag{16}$$

where $L$ is the number of layers, $H_j^{(L)}$ denotes the output of the final layer for the $j$th subset in the $L$th layer, $X_j^{(L)}$ represents the input data matrix for the $j$th subset in the $L$th layer, $W_j^{(L)}$ is the final weight matrix for the $j$th subset in the $L$th layer, $b_j^{(L)}$ is the final bias vector for the $j$th subset in the $L$th layer. The output weights for each meta-sub-ELM group are determined as given by

$$\beta_j^{(L)} = H_j^{\dagger(L)} T_j. \tag{17}$$

where $T_j$ denotes the target data vector for the $j$th subset, $H_j^{\dagger(L)}$ is the inverse matrix of $H_j^{(L)}$, and $\beta_j^{(L)}$ represents the output weights for the $j$th subset in the $L$th layer. For each sub-meta ELM group in the final layer, the output $H^{(L)}$ is calculated according to Eq. (12) for all input data received from the preceding layer. These outputs are then summed and the final output of the model is obtained using the Kernel matrix.

$$Y = \Omega^{(L)} \left(\frac{I}{C^{(L)}} + \Omega^{(L)}\right)^{-1} \cdot T. \tag{18}$$

In this equation, $Y$ denotes the ML-MetaKELM model output and $\Omega^{(L)}$ is the Kernel matrix for the last layer.

## 3. Experimental results and forecasting performance analysis

### 3.1. Tidal data description

In this study, two distinct real-world tidal datasets from geographically different locations were utilized to evaluate the model's performance across diverse tidal characteristics. The primary dataset, sourced from the AP Buoy in the Gulf of Mexico (latitude 27° 47.543' N, longitude 96° 57.392' W, depth 20 m) [31], was used to test the model. This dataset, provided by the National Oceanic and Atmospheric Administration (NOAA), consists of 6-minute tidal current measurements for one month for each season months (January, April, July, and October 2022), capturing seasonal variations. The second dataset, obtained from the Shark River Entrance in Florida of U.S. (latitude 25° 20.7 N, longitude 81° 7.6 W, depth 0.58 m), was used to validate the model's generalizability. This dataset, provided by NOAA [31], includes 6-minute readings from October 1–25, 1999, and has been previously used in the literature for tidal forecasting analysis [32].

Table 1 presents the descriptive statistical values of the and the second dataset, including the mean, standard deviation, maximum, minimum, Skewness, Kurtosis, and median, are presented. It can be seen from the results that the datasets exhibit both similarities and differences in their statistical characteristics across the datasets. For instance, while the mean values range from 15.95 in July to 35.08 in April, the standard deviations vary between 9.24 in July and 19.42 in April. Moreover, the Skewness values indicate slight asymmetry in all datasets, with April and October showing more pronounced positive

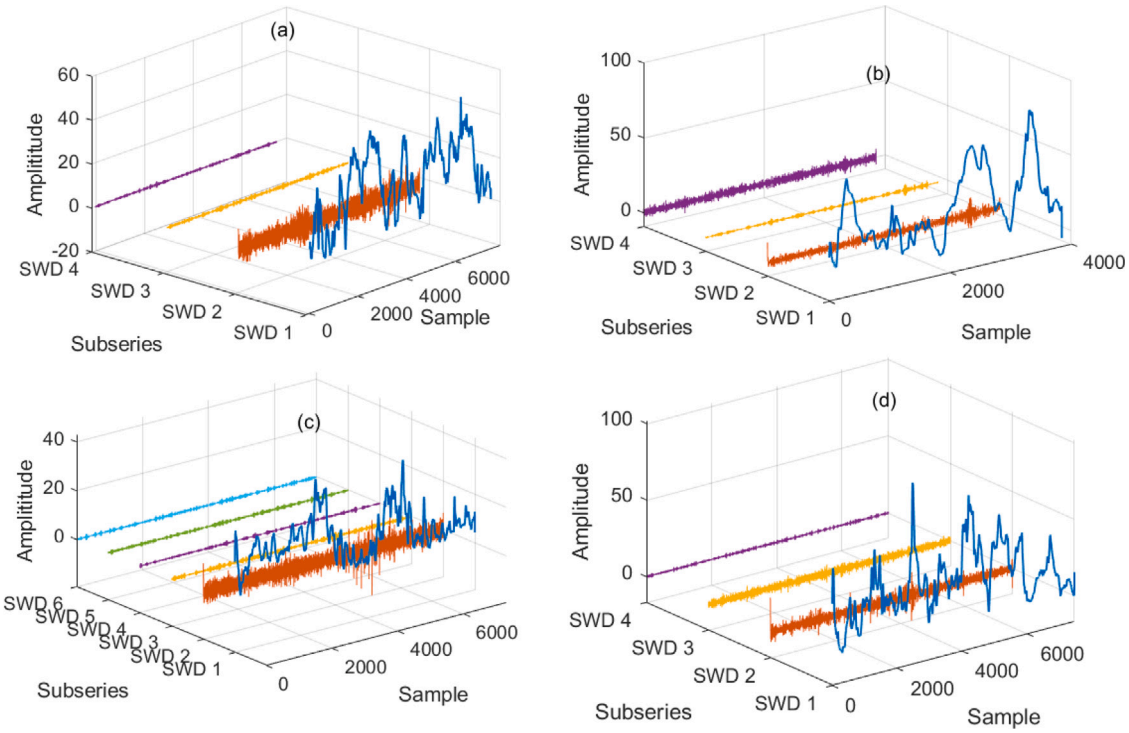


**Fig. 2.** Decomposition of the tidal current data from each season's representative months based on the SWD approach, (a) January, (b) April, (c) July, (d) October.

**Table 1**
The statistical parameters of the tidal current dataset used for representative months from each season [31].

| Dataset | Max. value | Min. value | Mean | Std. | Skewness | Kurtosis | Median |
|---|---|---|---|---|---|---|---|
| January | 65.3 | 0.1 | 26.28 | 13.54 | 0.04 | 1.98 | 26.5 |
| April | 99.4 | 0.9 | 35.08 | 19.42 | 0.71 | 2.67 | 30.1 |
| July | 48.0 | 0.1 | 15.95 | 9.24 | 0.58 | 2.82 | 15.0 |
| October | 107.2 | 0.2 | 31.24 | 17.88 | 0.72 | 3.67 | 29.2 |
| Shark River Dataset | 141.5 | 0.2 | 61.98 | 28.48 | −0.09 | 2.42 | 62.5 |

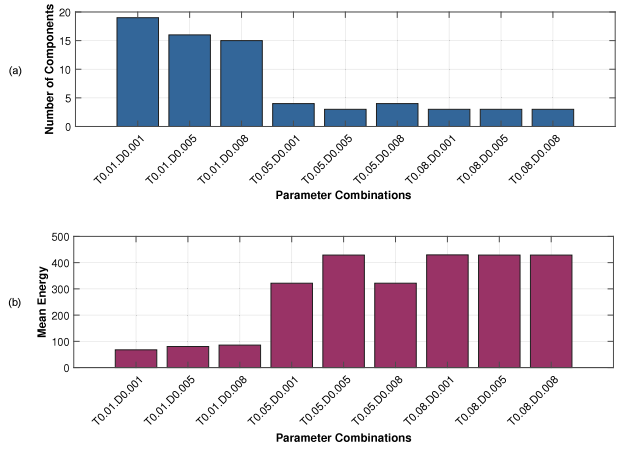


**Fig. 3.** Sensitivity analysis for combinations of SWD parameters, (a) number of components (b) mean energy.

skewness. The Kurtosis values suggest varying levels of peakedness, particularly in October, which has the highest Kurtosis value. Notably, the Shark River Dataset exhibits the highest mean (61.98) and maximum value (141.5), indicating significantly higher tidal variations compared to the seasonal datasets. These statistical variations across the datasets allow for a comprehensive evaluation of the adaptability of the proposed model.

### 3.2. Sensitivity analysis of SWD parameters

To evaluate the sensitivity of SWD parameters, two critical values were performed using tidal data: threshold for component extraction (cmps thresh) and threshold for iterative refinement (detail depth). Sensitivity analysis was performed to examine the number of components extracted and the mean energy of the components under various combinations of these parameters. Notably, changes in the number of components influence the level of signal decomposition and computational cost, whereas the mean energy serves as a critical metric for evaluating the information-carrying capacity of the extracted components. According to the SWD methodology, the cmps thresh value controls the threshold for extracting oscillatory modes from the signal. Smaller values of cmps thresh enable finer decompositions with more components extracted, whereas larger values yield coarser decompositions, focusing on dominant components. The detail depth parameter determines the precision of iterative refinements during the decomposition process; lower values ensure detailed refinements, while higher values provide faster convergence with potentially fewer components.

Fig. 3 presents the impact of these combinations of parameters on the number of components and the mean energy of the decomposed signals. The analyzed parameter ranges were set as cmps thresh values of $[0.01, 0.05, 0.08]$ and detail depth values of $[0.001, 0.005, 0.008]$. These parameter combinations were abbreviated as T (for cmps thresh) and D (for detail depth), with labels like T0.01.D0.001 and T0.08.D0.008 displayed on the x-axes of the sensitivity analysis results. The results shows that the number of decomposed components decreases as the T (cmps thresh) and D (detail depth) values increase, eventually reaching the same number of subcomponents beyond a certain point. Considering computational cost alongside the average energy levels, T = 0.05 and D = 0.005 were identified as the optimal parameter values. In Fig. 4, the reconstructed signals for each parameter combination are compared with the original signal. Although the number of decomposed signals increases with smaller cmps thresh and detail depth values, Fig. 4 shows that no significant data loss occurs in the reconstructed signals. This ensures that the method maintains the integrity of the original tidal

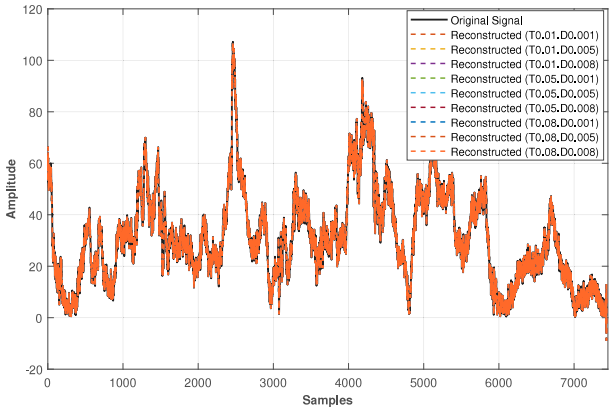


**Fig. 4.** Original and reconstructed signals for each parameters.

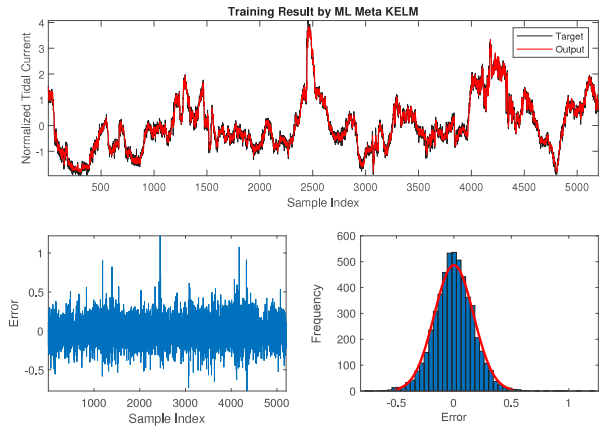


**Fig. 5.** Comparison of the train performance results.

current data while allowing a detailed examination of its components. For all conducted analyses, the sensitivity results were carefully considered to select the most suitable and optimal parameter configuration. The results highlight that both cmps thresh and detail depth values significantly influence the number and energy of the extracted components, as well as the accuracy of the reconstructed signals. It is therefore concluded that the selection of SWD parameters is critical to achieve accurate and physically meaningful results in tidal current forecasting.

### *3.3. Testing, validation, and performance analysis of the proposed hybrid model*

The analysis of the proposed model includes three key stages: decomposition, forecasting, and aggregation. Firstly, the SWD approach is applied to the original tidal current data to capture the full details of the current signal. Importantly, during the SWD process, no data is lost from the original signal; in other words, the original data can be fully reconstructed by aggregating the SWD-decomposed signals. The decomposition results for the original signals from each season's representative months are shown in Fig. 2. The number of sub-components varies based on the data's characteristics. Notably, the SWD1 component captures core features of the tidal current data. The forecasting accuracy of this component is critical, as it significantly influences the final aggregated prediction performance.

Before the forecasting step, the decomposed signals are divided into training and testing sets with a 70:30 ratio. Using historical data, input sets for training and testing are generated through the sliding window technique. This method requires careful selection of the window width, as it plays a crucial role in defining the optimal model structure by accounting for the relationship between current values and past time series data. The decomposed signals individually feed into separate ML-MetaKELM models, allowing each component to be specifically modeled in the forecasting process. The ML-MetaKELM model enables information transfer between layers in a deep-learning-inspired structure, using kernel-based transformations at each layer and processing data divided into smaller subsets. This model adopts an auto-encoder-like approach, where each layer derives progressively higher-level representations of the input data and passes them to the subsequent layer. The architecture consists of L distinct layers, with each layer partitioning the input data into M subsets. Each subset independently determines its hidden layer weights and applies kernel transformations, allowing for learning within each layer. The outputs from each layer then serve as inputs for the next, refining the data representation with each progression. Initially, hidden layer weights and bias values are randomly assigned within the Meta sub-ELM groups, enhancing variability in each layer's learning process. The model's training performance is shown in Fig. 5.

The top panel of Fig. 5 presents a comparison between the predicted outputs of the model and the target values while the subsequent panels show an error analysis, including metrics such as the MSE, the RMSE, the mean error, and the standard deviation. With a mean squared error of 0.0292 and a root mean squared error of 0.1709, the model demonstrates strong learning performance on the input data during the training phase. The mean error is also close to zero, highlighting the minimal bias in the model's predictions and confirming its precision in capturing tidal current trends. This training performance serves as a foundation for the subsequent forecasting phase, where monthly analyses are conducted to compare the results of this standalone model with those from the hybrid model incorporating SWD decomposition results.

To evaluate the forecasting performance of the proposed model, well-established numerical metrics such as RMSE, MSE, MAE, and $R^2$ were employed. While traditional metrics are widely used, they have several limitations. For instance, RMSE penalizes larger errors more heavily due to the squaring of residuals, which can disproportionately influence the metric, especially in datasets with outliers. $R^2$ may provide less reliable results for non-linear models or datasets with significant variability. To address these shortcomings, the $CV$ was included to provide a normalized measure of variability relative to the mean tidal current values. Lower $CV$ values indicate better model performance, and it is mathematically expressed as:

$$CV = \frac{\frac{1}{N}\sqrt{\sum_{i=1}^{N}\left(y_i - \tilde{y}_i\right)^2}}{\bar{y}_i}. \tag{19}$$

The analysis evaluates the forecasting accuracy of the proposed model using representative months from each season, comparing its performance against other ELM-based models and LSTM, a widely used deep learning method. Table 2 presents these comparative results, demonstrating that the proposed model consistently outperforms the other models. Across all evaluated months, the proposed model achieves notably lower error metrics and higher $R^2$ values. For instance, in October, the proposed model achieves significantly lower error metrics than the other methods, with an RMSE of 1.2155, an MSE of 1.4775, an MAE of 0.8882, a CV of 0.0543, and an $R^2$ value of 0.9933. Similarly, in other months, the proposed model consistently shows lower error values lower CV values, such as 0.068 in April and 0.0902 in January, and higher $R^2$ values, indicating improved forecasting accuracy. Notably, in the analyses for January and July, the proposed model outperforms both LSTM and other ELM-based models. For example, in July, the proposed model achieves a CV value of 0.2035, which is substantially lower than LSTM (0.2067) and other models, highlighting its stability and precision in forecasting. These results highlight the proposed model's superior accuracy and reliability and reduced variability in predicting tidal current data across various months.

**Table 2**
Performance comparison of the proposed model against other ELM-based models, and LSTM across representative months from each season.

| | | RMSE | MSE | MAE | $R^2$ | CV |
|---|---|---|---|---|---|---|
| October | Meta ELM | 2.7707 | 7.677 | 2.1855 | 0.9653 | 0.1238 |
| | Meta Kernel ELM | 2.611 | 6.8173 | 2.0625 | 0.9692 | 0.1167 |
| | ML Meta KELM | 2.6216 | 6.8725 | 2.0721 | 0.9689 | 0.1172 |
| | LSTM | 2.7569 | 7.6003 | 2.1984 | 0.9656 | 0.1232 |
| | Proposed | **1.2155** | **1.4775** | **0.8882** | **0.9933** | **0.0543** |
| April | Meta ELM | 3.8263 | 14.6408 | 2.7418 | 0.9669 | 0.1079 |
| | Meta Kernel ELM | 3.7259 | 13.8821 | 2.6883 | 0.9686 | 0.1051 |
| | ML Meta KELM | 4.0263 | 16.211 | 2.7983 | 0.9634 | 0.1136 |
| | LSTM | 3.8085 | 14.5044 | 2.7828 | 0.9672 | 0.1074 |
| | Proposed | **2.4121** | **5.8183** | **1.2897** | **0.9869** | **0.0680** |
| January | Meta ELM | 3.1401 | 9.8601 | 2.4061 | 0.9414 | 0.1170 |
| | Meta Kernel ELM | 3.0045 | 9.0272 | 2.3175 | 0.9463 | 0.1120 |
| | ML Meta KELM | 2.9808 | 8.8852 | 2.3021 | 0.9472 | 0.1111 |
| | LSTM | 4.4391 | 19.7059 | 3.5692 | 0.8829 | 0.1654 |
| | Proposed | **2.4193** | **5.8532** | **1.8832** | **0.9652** | **0.0902** |
| July | Meta ELM | 2.8808 | 8.2989 | 2.1929 | 0.8031 | 0.2738 |
| | Meta Kernel ELM | 2.8414 | 8.0733 | 2.1589 | 0.8084 | 0.2701 |
| | ML Meta KELM | 2.8675 | 8.2225 | 2.1739 | 0.8049 | 0.2726 |
| | LSTM | 2.1754 | 4.7322 | 1.6662 | 0.8877 | 0.2067 |
| | Proposed | **2.1403** | **4.5808** | **1.6054** | **0.8913** | **0.2035** |

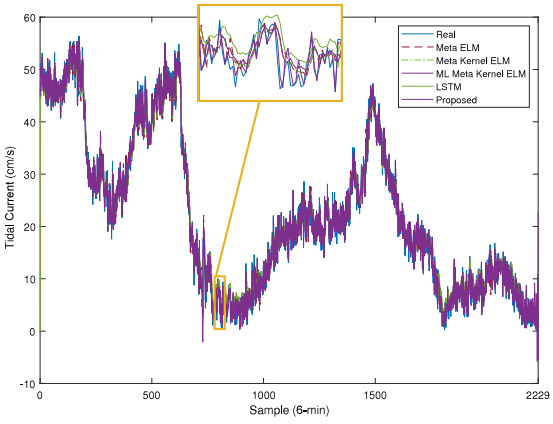


**Fig. 6.** Forecasting test results of the implemented models for October.

Fig. 6 through Fig. 9 present the forecasting test results for the implemented models across the representative months of October, April, January, and July. Each figure compares the forecasted tidal current values from the proposed model with those from Meta ELM, Meta Kernel ELM, ML Meta Kernel ELM, and LSTM, along with the actual data. Across all months, the proposed model consistently demonstrates a closer alignment with the real tidal current values, outperforming the other models in tracking variations in the tidal current data. This is particularly evident in October (see Fig. 6), April (see Fig. 7), and January (see Fig. 8) where the proposed model shows significantly reduced deviation from actual values. The performance metrics in each figure highlights the robustness of the proposed model, as it maintains low error rates and high accuracy even with seasonal fluctuations. These results indicate that the proposed model not only captures seasonal trends but also adapts well to the complex nature of tidal current patterns, proving its efficacy over ELM-based models and LSTM in predicting tidal currents with higher precision.

Considering these figures and performance metric results in Table 2, the integration of the SWD decomposition method into the ML-MetaKELM model further strengthens the forecasting performance by enhancing the model's ability to capture complex patterns within tidal current data. SWD enables the model to decompose original signals into distinct oscillatory components, effectively reducing noise and improving

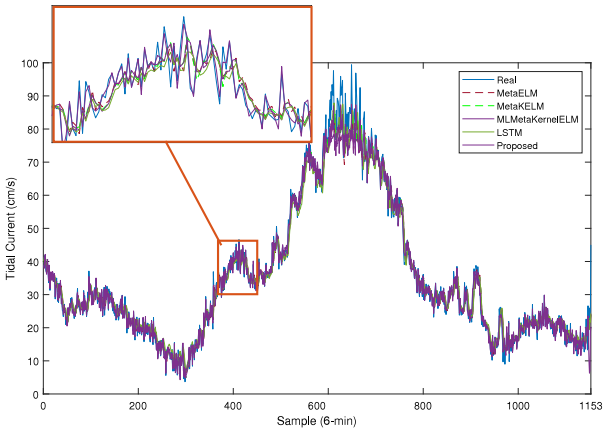


**Fig. 7.** Forecasting test results of the implemented models for April.

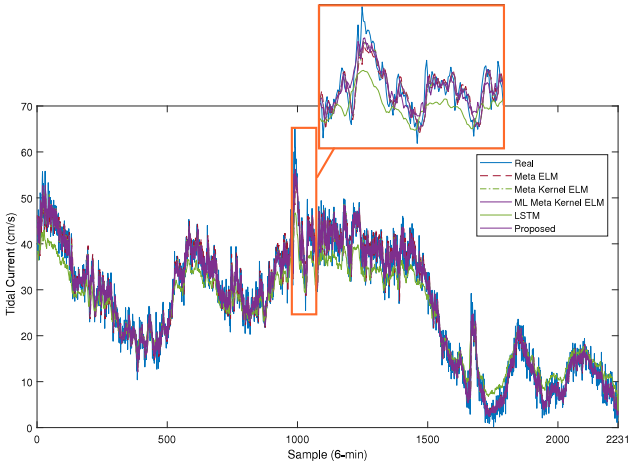


**Fig. 8.** Forecasting test results of the implemented models for January.

feature extraction. This decomposition-based approach improves the quality of inputs for ML-MetaKELM, allowing it to focus on critical features within each component and thus achieve superior accuracy and robustness. As a result, the combined SWD and ML-MetaKELM methodology demonstrates significant improvements over standalone models and the LSTM, maintaining high forecasting performance even among seasonal fluctuations.

The performance of the proposed model was further validated using a distinct tidal dataset from the Shark River Entrance (Florida, U.S.) [32]. It is worth noting that while this dataset originates from the same location, differences in data collection depths preclude a direct comparison of results. As such, the findings presented here should be interpreted within this context. As reported in Table 3, the proposed model achieved significantly better performance compared to other ELM-based models and the LSTM. Notably, it recorded the lowest error metrics, including an RMSE of 2.82, MSE of 7.96, MAE of 1.90, and CV of 0.0434, as well as the highest $R^2$ value of 0.9920. These results highlight the model's capability to accurately capture the complex tidal patterns and dynamic variations present in a geographically and temporally distinct dataset.

The analysis demonstrates that the integration of Swarm Decomposition (SWD) with the ML-MetaKELM enhances the model's robustness and adaptability to varying tidal characteristics. Compared to the other models, the proposed approach effectively isolates and processes the oscillatory components, leading to superior feature extraction and improved forecasting accuracy. For instance, the LSTM model showed relatively higher errors, with an RMSE of 9.24 and CV of 0.1423,

**Table 3**
Performance comparison of the proposed model with other ELM-based models and LSTM on the second tidal current dataset from a distinct geographic location [32].

| | | RMSE | MSE | MAE | $R^2$ | CV |
|---|---|---|---|---|---|---|
| Shark River Dataset | Meta ELM | 5.5686 | 31.0094 | 4.2238 | 0.9692 | 0.0857 |
| | Meta Kernel ELM | 5.2567 | 27.6338 | 4.0009 | 0.9725 | 0.0809 |
| | ML Meta KELM | 5.2024 | 27.0656 | 3.9957 | 0.9731 | 0.0801 |
| | LSTM | 9.2433 | 85.4393 | 7.8094 | 0.9151 | 0.1423 |
| | Proposed | **2.82143** | **7.9605** | **1.89613** | **0.9920** | **0.0434** |

showing its limitations in handling multi-frequency and non-stationary tidal signals. Similarly, traditional ELM-based models exhibited moderate performance but were outperformed by the proposed model in all evaluated metrics. These findings validate the generalizability of the proposed model, highlighting its ability to adapt to different tidal environments while maintaining high forecasting accuracy.

In the last stage of the experiments, this paper evaluates the forecasting models' performance by calculating tidal power values derived from a standardized tidal-stream power curve. This approach allows for an assessment of how forecasting accuracy impacts power output, highlighting the potential errors or deviations in power calculations introduced by each model. To obtain the power from tidal current data, the standardized power curve in [33], based on mean values of 14 commercial devices is performed according to Eq. (20).

$$P_t = \begin{cases} 0, & u < 0.3V_r \\ 0.185u^3 \cdot A, & 0.3V_r \le u \le V_r, \\ P_r, & u > V_r \end{cases} \tag{20}$$

where $V_r$ and $P_r$ represent the rated speed and power, respectively. The tidal power, $P_t$ is a related cubic function of the current velocity ($u$) over the rotor-swept area, $A$. To calculate the tidal power from current, these parameter in this paper are determined according to [34]. To ensure a more accurate power estimation without changing the inherent characteristics of the data, the amplitude of the current velocity data was increased ten-fold during power calculations. This adjustment provides a clearer depiction of the forecasting models' impact on power output predictions. Fig. 10 presents a comparative analysis of power forecasting derived from the tidal current data, emphasizing both the highest and lowest-performing models. The proposed model achieved the best-performance with an MAE of 119.51 kW, while the LSTM demonstrated the worst performance with the highest MAE of 300.77 kW. This marks approximately a 60% improvement in accuracy. Such a significant reduction in error emphasizes the impact of selecting an optimal forecasting model, as it enhances the reliability of tidal power predictions and reduces potential discrepancies in power output, and ultimately supports more stable and efficient grid operations.

## 4. Conclusions

This study proposed an innovative hybrid model, integrating SWD with a Kernel-based Multi-Layer Meta-ELM (ML-MetaKELM), to enhance the accuracy and computational efficiency of tidal current-to-power forecasting. Addressing the challenges inherent in predicting complex, non-stationary tidal signals, the SWD technique effectively decomposes tidal current data into oscillatory components, significantly reducing noise and improving feature extraction. The architecture of MetaKELM, improves generalization and reduces the need for extensive parameter tuning. This makes the proposed solution scalable solution suitable for diverse tidal forecasting applications.

To validate the robustness of the proposed model, we conducted a sensitivity analysis of key SWD parameters. This analysis demonstrated the impact of parameter choices on decomposition quality and computational efficiency, confirming the model's adaptability to diverse signal

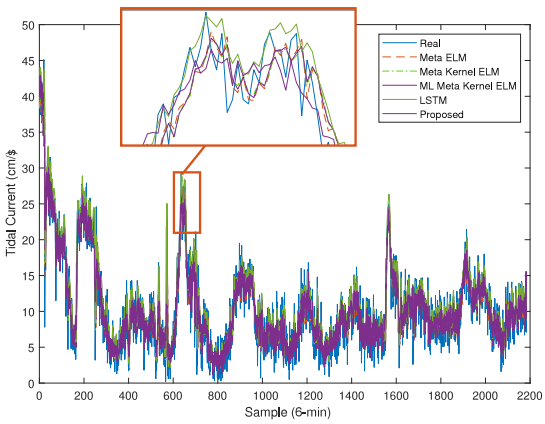


**Fig. 9.** Forecasting test results of the implemented models for July.

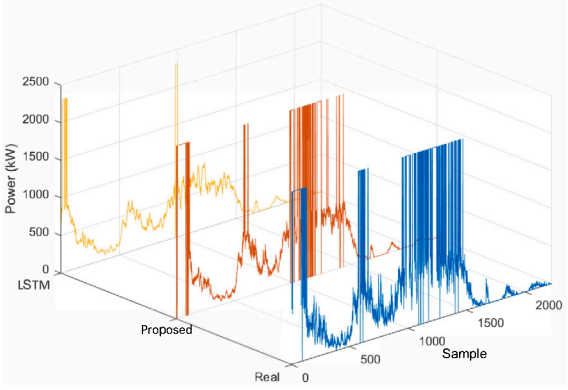


**Fig. 10.** The effect of forecasting model performance on tidal power.

characteristics. The model was tested on two tidal current datasets geographically and temporally distinct locations to demonstrate its capability to adapt to varying tidal environments. The performance was comparatively evaluated against other ELM-based and LSTM models from the literature. The model consistently outperformed other ELM-based models and LSTM in both datasets, achieving lower error metrics (*e.g.*, RMSE, MSE, MAE, and CV) and higher $R^2$ values. The study further validated the model's effectiveness by evaluating its impact on tidal power prediction, showing a 60% improvement in accuracy over LSTM. This substantial reduction in forecasting error highlights the importance of optimal forecasting models for tidal power applications, as greater accuracy in tidal current forecasts translates directly into more reliable power output predictions, supporting the stable and efficient design and management of power processing and storage systems.

This study employs a standardized tidal-stream power curve, derived from the mean values of 14 commercial devices, to assess power output. While this approach provides a practical framework for large-scale evaluations, it does not account for device-specific variability, which could be addressed in future research. Future directions also include exploring metaheuristic optimization techniques and large language model-based approaches to further improve forecasting accuracy and scalability. Extending the model's adaptability to real-time forecasting across broader geographic regions and varying environmental conditions remains a key goal.

## CRediT authorship contribution statement

**Emrah Dokur:** Writing – review & editing, Writing – original draft, Validation, Software, Methodology, Formal analysis, Data curation, Conceptualization. **Nuh Erdogan:** Writing – review & editing, Writing

– original draft, Validation, Supervision, Methodology, Investigation, Formal analysis, Data curation, Conceptualization. **Ugur Yuzgec:** Writing – review & editing, Writing – original draft, Validation, Supervision, Software, Methodology, Formal analysis, Data curation, Conceptualization.

## Declaration of competing interest

The authors declare that they have no known competing financial interests or personal relationships that could have appeared to influence the work reported in this paper.

## Acknowledgment

The authors acknowledges the invaluable support and resources provided by the Marine Renewable Energy Centre of Ireland (MaREI) at University College Cork (UCC), Ireland. The foundational infrastructure and expertise developed during Authors' postdoctoral research tenure at MaREI significantly contributed to the knowledge and tools applied in this study.

## References

[1] E. Dokur, N. Erdogan, M.E. Salari, U. Yuzgec, J. Murphy, An integrated methodology for significant wave height forecasting based on multi-strategy random weighted grey wolf optimizer with swarm intelligence, IET Renew. Power Gener. 18 (3) (2024) 348–360.
[2] B.P. Hand, N. Erdogan, D. Murray, P. Cronin, J. Doran, J. Murphy, Experimental testing on the influence of shaft rotary lip seal misalignment for a marine hydro-kinetic turbine, Sustain. Energy Technol. Assessments 50 (2022) 101874.
[3] IRENA (2020), Ocean energy stats & trends 2023., 2024, URL: https://www.oceanenergy.eu.
[4] P. Qian, B. Feng, X. Liu, D. Zhang, J. Yang, Y. Ying, C. Liu, Y. Si, Tidal current prediction based on a hybrid machine learning method, Ocean Eng. 260 (2022) 111985.
[5] A. Kavousi-Fard, A hybrid accurate model for tidal current prediction, IEEE Trans. Geosci. Remote Sens. 55 (1) (2016) 112–118.
[6] H.H. Aly, A novel approach for harmonic tidal currents constitutions forecasting using hybrid intelligent models based on clustering methodologies, Renew. Energy 147 (2020) 1554–1564.
[7] N. Pinardi, P.F. Lermusiaux, K.H. Brink, R.H. Preller, The sea: The science of ocean prediction, J. Mar. Res. 75 (2017) 189–237.
[8] K.Y. Kareem, Y. Seong, K. Kim, Y. Jung, A case study of tidal analysis using theory-based artificial intelligence techniques for disaster management in Taehwa River, South Korea, Water 14 (14) (2022) 2172.
[9] K. Zhang, X. Wang, H. Wu, X. Zhang, Y. Fang, L. Zhang, H. Wang, Study of the performance of deep learning methods used to predict tidal current movement, J. Mar. Sci. Eng. 11 (1) (2022) 26.
[10] A.M. Mihel, J. Lerga, N. Krvavica, Estimating water levels and discharges in tidal rivers and estuaries: Review of machine learning approaches, Environ. Model. Softw. (2024) 106033.
[11] C.-H. Yang, C.-H. Wu, C.-M. Hsieh, Y.-C. Wang, I.-F. Tsen, S.-H. Tseng, Deep learning for imputation and forecasting tidal level, IEEE J. Ocean. Eng. 46 (4) (2021) 1261–1271.
[12] M. Qin, Z. Li, Z. Du, Red tide time series forecasting by combining ARIMA and deep belief network, Knowl.-Based Syst. 125 (2017) 39–52.
[13] C.-H. Yang, C.-H. Wu, C.-M. Hsieh, Long short-term memory recurrent neural network for tidal level forecasting, IEEE Access 8 (2020) 159389–159401.
[14] A. Das, W. Kong, A. Leach, S. Mathur, R. Sen, R. Yu, Long-term forecasting with tide: Time-series dense encoder, 2023, arXiv preprint arXiv:2304.08424.
[15] A. Kavousi-Fard, Modeling uncertainty in tidal current forecast using prediction interval-based SVR, IEEE Trans. Sustain. Energy 8 (2) (2016) 708–715.
[16] M. Balci, E. Dokur, U. Yuzgec, N. Erdogan, Multiple decomposition-aided long short-term memory network for enhanced short-term wind power forecasting, IET Renew. Power Gener. 18 (3) (2024) 331–347.
[17] T. Monahan, T. Tang, T.A. Adcock, A hybrid model for online short-term tidal energy forecasting, Appl. Ocean. Res. (ISSN: 0141-1187) 137 (2023) 103596.
[18] Q. Wu, H. Yang, G. Li, Energy fluctuation pattern recognition coupled with decomposition-integration: A novel ocean tidal energy forecasting system, Measurement 238 (2024) 115374.
[19] S.M.J. Jalali, S. Ahmadian, M.K. Noman, A. Khosravi, S.M.S. Islam, F. Wang, J.P. Catalão, Novel uncertainty-aware deep neuroevolution algorithm to quantify tidal forecasting, IEEE Trans. Ind. Appl. 58 (3) (2022) 3324–3332.
[20] W. Ban, L. Shen, F. Lu, X. Liu, Y. Pan, Research on long-term tidal-height-prediction-based decomposition algorithms and machine learning models, Remote. Sens. 15 (12) (2023) 3045.
[21] T. Cheng, Y. Dong, Y. Huang, A tidal current speed forecasting model based on multiple periodicity learning, 2024, arXiv Preprint arXiv:2410.09718.
[22] V.K. Rayi, S. Mishra, J. Naik, P. Dash, Adaptive VMD based optimized deep learning mixed kernel ELM autoencoder for single and multistep wind power forecasting, Energy 244 (2022) 122585.
[23] E. Dokur, N. Erdogan, M.E. Salari, C. Karakuzu, J. Murphy, Offshore wind speed short-term forecasting based on a hybrid method: Swarm decomposition and meta-extreme learning machine, Energy 248 (2022) 123595.
[24] Y. Miao, M. Zhao, V. Makis, J. Lin, Optimal swarm decomposition with whale optimization algorithm for weak feature extraction from multicomponent modulation signal, Mech. Syst. Signal Process. 122 (2019) 673–691.
[25] C. Xiao, J. Yu, Adaptive swarm decomposition algorithm for compound fault diagnosis of rolling bearings, IEEE Trans. Instrum. Meas. 72 (2023) 1–14.
[26] C.M. Wong, C.M. Vong, P.K. Wong, J. Cao, Kernel-based multilayer extreme learning machines for representation learning, IEEE Trans. Neural Netw. Learn. Syst. 29 (3) (2016) 757–762.
[27] J.A. Vásquez-Coronel, M. Mora, K. Vilches, A review of multilayer extreme learning machine neural networks, Artif. Intell. Rev. 56 (11) (2023) 13691–13742.
[28] R. Bisoi, P. Dash, P.P. Das, Short-term electricity price forecasting and classification in smart grids using optimized multikernel extreme learning machine, Neural Comput. Appl. 32 (2020) 1457–1480.
[29] J. Kamruzzaman, R.A. Sarker, I. Ahmad, SVM based models for predicting foreign currency exchange rates, in: Third IEEE International Conference on Data Mining, IEEE, 2003, pp. 557–560.
[30] J. Gui, Z. Sun, J. Cheng, S. Ji, X. Wu, How to estimate the regularization parameter for spectral regression discriminant analysis and its kernel version? IEEE Trans. Circuits Syst. Video Technol. 24 (2) (2013) 211–223.
[31] National Oceanic and Atmospheric Administration Tides and Current Data, Noaa, 2024, URL: https://tidesandcurrents.noaa.gov/.
[32] N. Safari, O.A. Ansari, A. Zare, C. Chung, A novel decomposition-based localized short-term tidal current speed and direction prediction model, in: 2017 IEEE Power & Energy Society General Meeting, IEEE, 2017, pp. 1–5.
[33] M. Lewis, R.O. Murray, S. Fredriksson, J. Maskell, A. de Fockert, S.P. Neill, P.E. Robins, A standardised tidal-stream power curve, optimised for the global resource, Renew. Energy 170 (2021) 1308–1323.
[34] Website 1, Sabella published turbine characteristics, Sabella, 2019, URL: https://www.sabella.bzh.